Road Materials and Pavement Design

ISSN: 1468-0629 (Print) 2164-7402 (Online) Journal homepage: http://www.tandfonline.com/loi/trmp20

Importance of binder modification type and aggregate structure on rutting resistance of asphalt mixtures using image-based multi-scale modelling

Cheng Ling, Amir Arshadi & Hussain Bahia

To cite this article: Cheng Ling, Amir Arshadi & Hussain Bahia (2016): Importance of binder modification type and aggregate structure on rutting resistance of asphalt mixtures using image-based multi-scale modelling, Road Materials and Pavement Design, DOI: 10.1080/14680629.2016.1189351

To link to this article: http://dx.doi.org/10.1080/14680629.2016.1189351

Published online: 26 May 2016.

Road Materials and Pavement Design, 2016
http://dx.doi.org/10.1080/14680629.2016.1189351

Taylor & Francis
Taylor & Francis Group

Importance of binder modification type and aggregate structure on rutting resistance of asphalt mixtures using image-based multi-scale modelling

Cheng Ling[a]*, Amir Arshadi[b] and Hussain Bahia[a]

[a]*Department of Civil and Environmental Engineering, University of Wisconsin – Madison, Madison, WI, USA;* [b]*College of Engineering, University of Oklahoma, Norman, OK, USA*

(*Received 26 December 2015; accepted 8 May 2016*)

Permanent deformation is known as one of the most critical distresses observed in asphalt pavements, and is known to depend on asphalt binder, aggregates and voids, which are the components of asphalt mixture. This study is an effort to investigate the effect of asphalt binder modification type and aggregate structure on rutting resistance through experimentation and finite-element simulation. Asphalt binders with different levels of non-recoverable compliance (Jnr) and elastic recovery (%*R*) based on the Multiple Stress Creep Recovery test were selected. Asphalt mixtures with different aggregate gradations were prepared for testing and image processing for numerical simulation. A flow number test was conducted on the mixture samples to obtain the asphalt mixture rutting performance. A two-dimensional (2D) image analysis was also conducted on the mixture samples to characterise their internal aggregate structures. In addition, a recently developed image-based multi-scale finite-element model was used to predict the permanent deformation of the asphalt mixtures. In this approach, four interconnected scales were modelled, namely asphalt binder, mastic, mortar and mixture scales through homogenisation and upscaling techniques to transfer the material properties from lower scale to higher scale. A novel approach for taking into account contact mechanics between aggregates as function of proximity is used at all scales. The simulation results show that by changing the aggregate gradation (packing), and the viscous component of asphalt binder (Jnr), the rutting resistance of asphalt mixtures can be significantly improved. However in comparison the elastic component of asphalt binder (% recovery) is not found to be a significant factor especially in a well-packed aggregate structure. The results raise questions about the focus by many agencies on the requirements of elastic recovery of binders as a tool to select modified binders for better high-temperature performance.

Keywords: MSCR; aggregate structure; multi-scale; elastic recovery; permanent deformation

Introduction

The Multiple Stress Creep and Recovery (MSCR) test (specified in standard test method AASHTO T350 and specification AASHTO M332), which is both performance based and blind to modification type (D'Angelo, Reinke, Bahia, & Marasteanu, 2010), was developed by FHWA as a replacement for the existing AASHTO M320 high-temperature asphalt binder test. The MSCR test uses the 1 s creep loading followed with the 9 s recovery over the multiple stress of 0.1 and 3.2 kPa at 10 cycles for each stress level. The average non-recovered strain for the 10 creep and recovery cycles is then divided by the applied stress for those cycles yielding the

*Corresponding author. Email: cling4@wisc.edu

non-recoverable compliance Jnr. Percent recovery (%*R*) is another important parameter from the MSCR test to reflect the elastic property of the asphalt binder, which is a measure of how much the sample returns to its initial shape after being repeatedly sheared and relaxed. The MSCR test has proved to be able to distinguish the difference in rutting potential between various binders, including both modified and unmodified binders, through numerous studies (D'Angelo et al., 2010). These findings indicated that the non-recoverable compliance Jnr is a good replacement for the SHRP high-temperature binder criteria and correlate well with the rutting resistance of asphalt mixture (D'Angelo et al., 2010; Gierhart, 2011).

However, it is not clear what the contributions of viscous component and elastic component of asphalt binder to the rutting resistance of the asphalt mixture are. The viscous and elastic components can be represented by Jnr and %*R*, respectively, obtained from the MSCR test. It is also not clear how much the asphalt binder properties could affect the aggregate structure during the compaction of mixtures, thus complicating the effects of all these factors on asphalt mixture high-temperature performances. Roohi, Tashman, and Bahia (2012) presented a study on testing and image analysis showing that the aggregate internal structure is important in rutting performance of asphalt mixture and that binder properties at compaction temperatures can significantly affects packing. Previous researches on the MSCR test indicated that the non-recoverable compliance Jnr can be correlated well with the mixture performance (D'Angelo et al., 2010; Gierhart, 2011). However, the relationship between asphalt binder elasticity and mixture rutting resistance performance is not clear yet and very limited research exists in studying the role of binder elasticity in asphalt mixture high-temperature performances. Golalipour (2011) found that a statistical relationship can be seen between the binder elasticity and mixture high-temperature performance but not significant due to the confounding effect of the change of aggregate structure based on limited data. He concluded that ensuring asphalt binder elasticity alone is not sufficient to improve rutting resistance of the mixture but it could be an important factor. Since it is very difficult to distinguish the effect of asphalt elastic and viscous properties and aggregate structures on the rutting resistance of asphalt mixtures through experimentation, this study considered modelling as an alternative tool to study the fundamental role of binders during repeated creep.

Recently, an image-based multi-scale modelling approach has been developed based on the finite-element (FE) method (Arshadi & Bahia, 2015). In this approach, four different scales were modelled, including asphalt binder, mastic, mortar and mixture scales (as shown in Figure 1). Homogenisation and upscaling techniques were used to transfer the material properties from lower scale to higher scale. The "mastic scale" contains fillers ranging from 1 μm up to 75 μm in a binder matrix; the "mortar scale" contains fine aggregates ranging from 75 μm to 1.18 mm in a mastic matrix, and the "mixture scale" contains all larger aggregates (those detected using

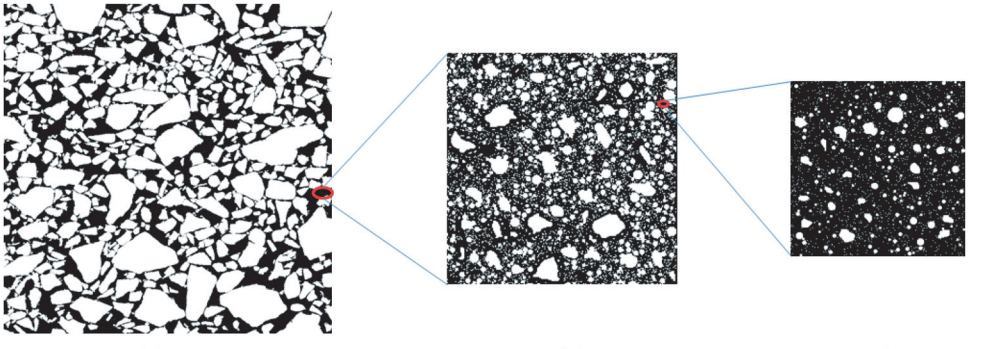

Figure 1. Multi-scale analysis scheme: (a) mixture scale, (b) mortar scale and (c) mastic scale.

simple 2D scanners and binary imaging filters) in a continuous mortar matrix. The data from the binder frequency sweep test were used to derive the binder master curve in the form of Prony Series. The binder properties were implemented into ABAQUS via the user material subroutine. The 2D artificial images of mastic and mortar were generated based on the real aggregate particle shapes, the aggregate distributions and volume fractions and characterised through FE simulations. The 2D scanned images of asphalt mixtures were then used by elimination of the fine particles and addition of the artificial air voids to study the asphalt mixture behaviour under creep and recovery loading. A simple particle-to-particle contact model was also proposed and used to transfer the effect of the particle contact at lower scale to the next higher scale through a nonlinear superposition method. The simulation results of the asphalt mixture matched well with the experimental test results after limited number of cycles, indicating the capability of this model in predicting the permanent deformation of asphalt mixtures at certain conditions.

The study reported in this paper utilises the image-based multi-scale approach developed in the previous research (Arshadi & Bahia, 2015) but adopts the MSCR test to provide the binder inputs instead of the frequency sweep test. Using the MSCR test result one can study directly the effect of the parameters Jnr and %*R* on the permanent deformation of asphalt mixtures. The modelling results were validated using the mixture performance test. In addition, mixtures with two levels of Jnr and %*R*, as well as two aggregate gradations, were included in the simulations to evaluate the effects of asphalt binder properties and aggregate structure on the simulated rutting resistance of asphalt mixtures.

Research objectives

This study is focused on utilising the image-based multi-scale modelling technique to investigate the effect of asphalt binder viscous/elastic properties and aggregate structure on the rutting resistance of asphalt mixtures under repeated creep and recovery loading. The primary objectives are as follows:

(1) Validate the simulation results of permanent deformation for a coarse and a fine asphalt mixtures using the multi-scale model. The inputs of the model include asphalt binder test data from the MSCR test, asphalt mix design information and mixture planar images.
(2) Investigate the effect of binder viscous and elastic properties and aggregate structure on the permanent deformation of asphalt mixtures using this validated model.

Selection of materials

Four asphalt binders named as LJHR, HJHR, LJLR and HJLR (i.e. LJHR = Low Jnr, High %*R*), including one real binder modified by Styrene–Butadiene–Styrene (SBS) and three artificially created binders with two levels of Jnr (0.018 and 0.036 kPa^{-1}) and %*R* (32.6% and 65.3%) under stress level of 0.1 kPa were included in this study. The Jnr and %*R* values for all the binders were determined based on the MSCR test at 46°C since the asphalt mixture was tested at this temperature. The LJHR stands for the asphalt binder with low Jnr (0.018 kPa^{-1}) and high recovery (65.3%), and similarly for HJHR, LJLR and HJLR binders. Among the four binders, LJHR binder is the real tested binder with PG 76-22 which was modified by 3.2% of SBS with a PG64-22 base binder and then aged under the RTFO test.

Two significantly different gradations used in previous studies on internal aggregate structure (Coenen, 2011) were also used in this study, categorised as coarse and fine gradation as shown in Figure 2.

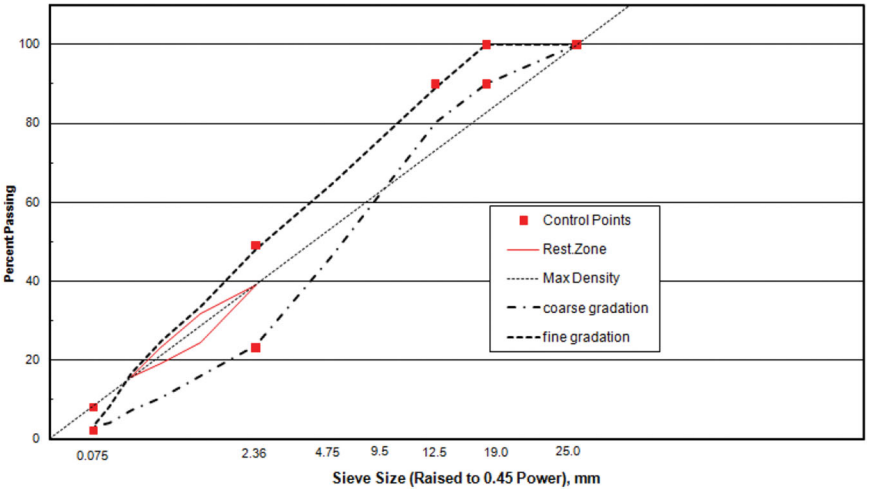

Figure 2. Gradations used in this study.

Fine- and coarse-graded mixtures with SBS-modified binder were designed and tested to validate the modelling results through the flow number test results. The asphalt contents were determined to be 4.62% and 5.55% for the fine and coarse mixtures, respectively, based on the Superpave mix design targeting the air voids of 4%. Then the flow number samples were prepared targeting the air voids of 7% based on the optimum asphalt content from the mix design. It should be noted that the same aggregate structures obtained for the fine- and coarse-graded mixtures with SBS-modified binder were used for the rest of the mixtures with three artificially generated binders in modelling to eliminate the confounding effect of aggregate structure when evaluating asphalt binder influence on permanent deformation of asphalt mixtures.

Test methods

Multi-scale analysis

The multi-scale analysis procedure developed in previous research (Arshadi & Bahia, 2015) was used in this study. Different steps of the multi-scale analysis are shown in Figure 3. It should be noted that instead of the frequency sweep test, the MSCR test was conducted on asphalt binders using Dynamic Shear Rheometer to obtain the Prony series parameters as input properties for ABAQUS. The MSCR test was selected so that one can obtain the viscous and elastic properties directly from the test. The detailed analysis procedure is discussed as follows.

The volume fractions for the components at each scale are important in creating the mastic and mortar images using the MATLAB-generated program. The calculated volume fractions of all the components at each scale are presented in Table 1. The air voids were included in the mixture scale.

The linear viscoelasticity assumption was followed in this study so that the Boltzmann Superposition Integral can be used as the constitutive relationship for asphalt binder. Therefore, only the MSCR test results at 0.1 kPa were considered. The MSCR test was performed following the AASHTO T350 procedure and the first 10 cycles at 0.1 kPa were fitted using the Burger's model, which is a commonly used phenomenological model to describe the creep and recovery behaviour of asphalt binder. The fitting results for the SBS-modified binder are presented in Figure 4(a). By applying Laplace transformation to Boltzmann Integrals, manipulating terms

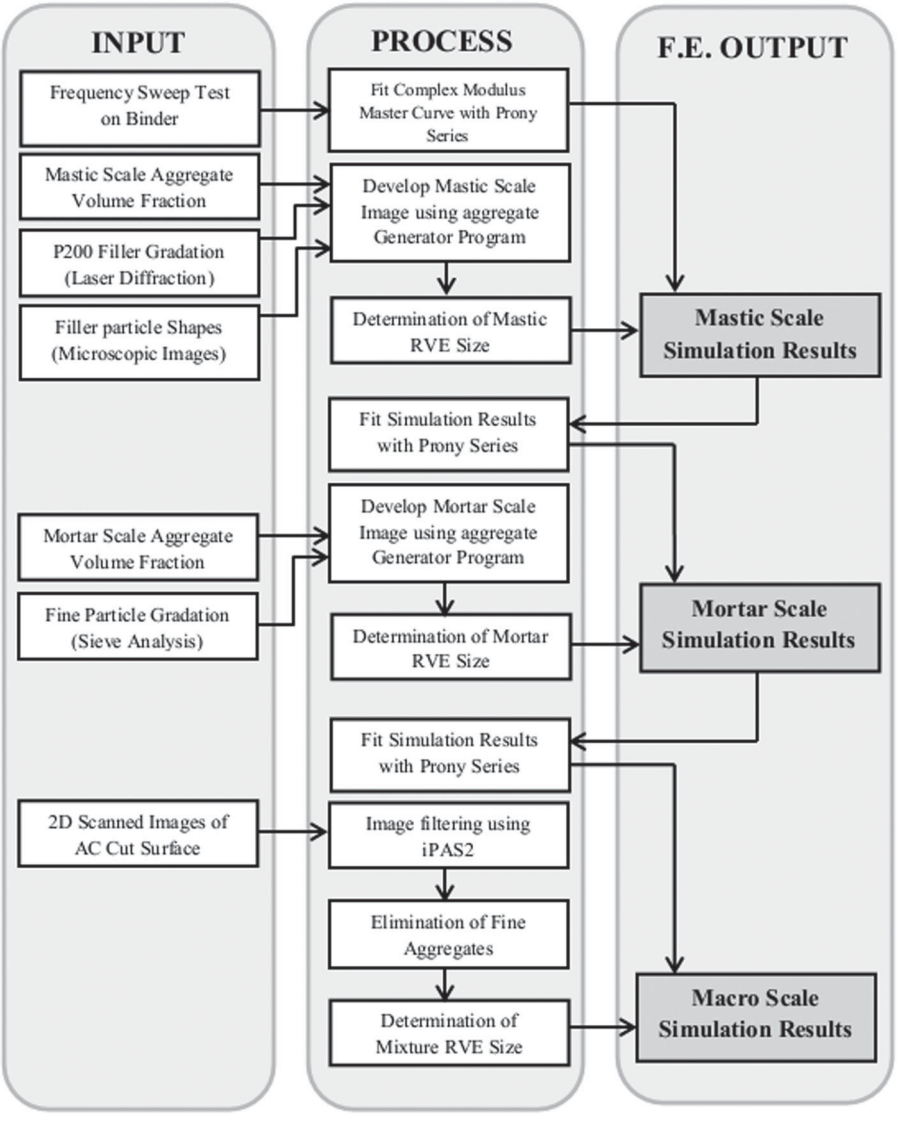

Figure 3. Flowchart of the multi-scale analysis procedure.

and applying another inverse Laplace transformation, the creep compliance obtained from the Burger's model can be converted and presented in terms of the Prony series relaxation modulus to be entered into ABAQUS (Kong & Yuan, 2010). Finally, the shear relaxation moduli in the Prony series were converted to elastic relaxation moduli using the Poisson's ratio of 0.49 for asphalt binders. The Burger's model parameters and converted elastic moduli of all four asphalt binders are presented in Figure 4(b). The numerical implementation was also performed on the one-dimensional linear constitutive model for asphalt binder based on the incremental finite-element modelling scheme with constant strain rate over each time increment proposed by Zocher et al. (Zocher, Groves, & Allen, 1997) to formulate the three-dimensional behaviour of asphalt binder.

Table 1. Volume fraction of component materials at each scale.

	Mixture scale			Mortar scale		Mastic scale	
Mixture type	Aggregate	Mortar	Air voids	Fine aggregates	Mastic	Fillers	Asphalt binder
Coarse	0.680	0.255	0.065	0.412	0.588	0.162	0.838
Fine	0.551	0.384	0.065	0.658	0.342	0.189	0.811

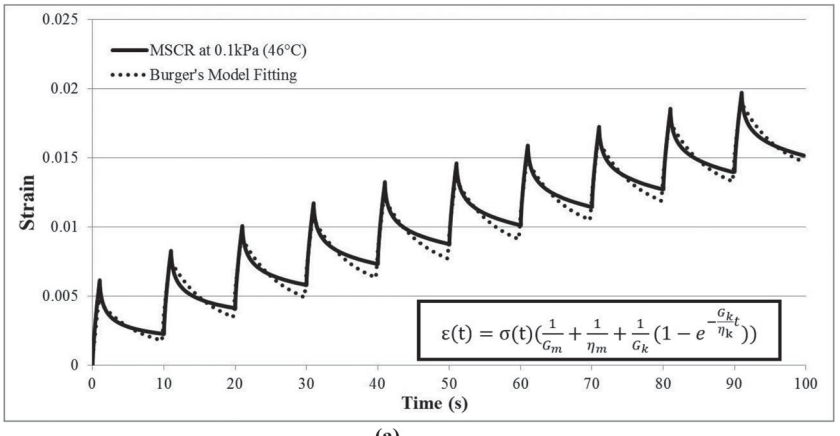

(a)

Binder Type		HJHR	HJLR	LJHR	LJLR
Burger's Model	G_m (Pa)	104769.63	209539.27	209539.27	419078.53
	η_m (Pa·s)	44768.91	44768.91	89537.82	89537.82
	G_k (Pa)	2242.80	2541.36	4485.60	5082.72
	η_k (Pa·s)	12342.78	37028.33	24685.56	74056.67
Prony Series	E_1 (Pa)	310199.17	626328.60	620398.33	1252657.20
	τ_1 (Pa·s)	0.0911	0.0964	0.0911	0.0964
	E_2 (Pa)	4109.73	2289.20	8219.47	4578.40
	τ_2 (Pa·s)	25.8006	32.3037	25.8006	32.3037

(b)

Figure 4. (a) Burger's model fitting of ten cycles at 0.1 kPa for the MSCR test at 46°C; (b) Burger's model and Prony series parameters fitted for all four binders.

The mastic binary image was created using a MATLAB-generated program based on the realistic shape of the filler particles, the particle gradation and the volume fraction of the fillers following the procedure developed in previous research (Arshadi & Bahia, 2015). The "Laser Diffraction" technique was used to experimentally determine the gradation of fillers and the realistic geometry of the filler particles was captured through microscopic imaging. The optimum represented volume element (RVE) size was determined to be a 225 × 225 μm area, approximately three times of the maximum size of filler particles. The details of determination of RVE can also be found in the previous research (Arshadi & Bahia, 2015). The same RVE was used for all subsequent analysis at the mastic scale. Two types of simulations were performed at the mastic scale: (a) frequency sweep to determine the complex modulus master curve at a low strain amplitude level to make sure that no contact happens and (b) creep loading test with/without applying the contact model for the aggregate particles to determine the strain-dependent contact function.

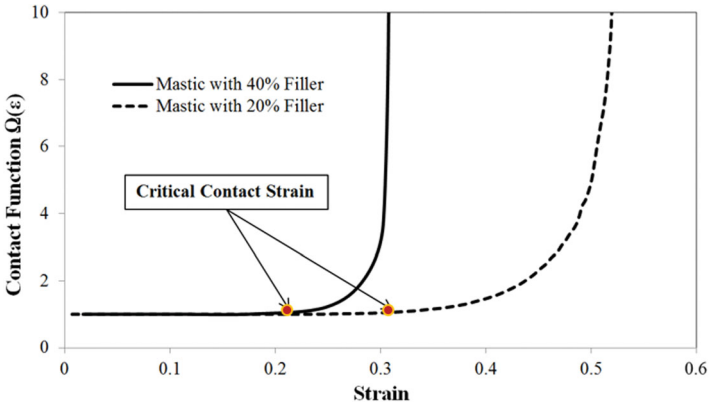

Figure 5. Illustration of contact function and critical contact strain.

The details of this analysis including the contact model and contact function can be found in the previous study (Arshadi & Bahia, 2015). In this study, the critical contact strain is defined as that at which the curve of the contact function starts increasing, as shown in Figure 5. The critical contact strain for the mastic with higher amount of filler is much lower than the one for the mastic with lower filler content, as illustrated in Figure 5, since the possibility of contact increases with filler content. The Poisson's ratio of the mastic was also determined during the creep loading simulation. The master curve of the mastic can be fitted using Prony series with one spring and three Maxwell elements to obtain the viscoelastic inputs of the continuous phase for the mortar scale. Similar to the mastic scale, the mortar image was generated based on the real aggregate shapes, gradation and volume fraction. The simulations to determine the master curve of mortar and particle contact function at the mortar scale were also performed.

To obtain the mixture image for simulation, the mixture sample was compacted and cut, and the section of the mixture was scanned using a flatbed scanner. A 2D image processing technique using iPas2 software which was developed by the University of Wisconsin (Coenen, 2011; Roohi et al., 2012) and successfully applied in coating research (Ling, Hanz, & Bahia, 2014; Ling, Moraes, Swiertz, & Bahia, 2013) was used to convert the coloured images to binary images. Due to the limitation of the resolution of the scanner, the aggregate with size smaller than 1.18 mm cannot be captured accurately. Therefore, those aggregates were eliminated from the mixture image using a MATLAB code and were considered at the lower scales. In addition, due to the lack of contrast between air voids and the asphalt in the mixture images, the artificially generated air voids were embedded into the image based on the bathtub shape distribution found by Masad, Jandhyala, Dasgupta, Somadevan, and Shashidhar (2002). The air voids were considered as empty spaces in ABAQUS simulation. Once the mixture image was prepared and imported into ABAQUS, a 70-cycle creep loading and recovery simulation with 0.1 s of loading time and 0.9 s of unloading time at each cycle was performed on the mixture to simulate the creep and recovery behaviour of asphalt mixture as experienced in the flow number test.

Image analysis

Roohi et al. found that specific microstructural indices such as total aggregate contact length in the aggregate skeleton represented by six 2D mixture section images show very good correlation with the flow number results (Roohi et al., 2012), indicating its effectiveness in evaluating the asphalt mixtures' high-temperature performance. In this study, the image analysis on the

coarse- and fine-graded mixtures with SBS-modified binder was performed to evaluate the internal aggregate structures. The procedures are presented in detail in Roohi et al. (2012) and briefly described as follows.

The samples were cut after compaction and the sections of the mixture were scanned. The image analysis was performed for aggregate structural characterisation using image processing software iPas2 (Roohi et al., 2012). The output index from the analysis is the total contact length which represents the packing condition in the asphalt mixture. Higher total contact length represents higher aggregate interlock and packing in the mixture thus resulting in better rutting resistance.

Flow number test

The repeated creep loading and recovery test (commonly known as flow number test) specified in AASHTO TP79 was used in this study to evaluate the rutting performance of the two mixtures with different gradations and validate the modelling results with the experimental data. The unconfined condition and the stress level of 345 kPa were selected. The test was conducted at 46°C on the sample with a diameter of 100 mm and a height of 150 mm compacted to the target air voids of 7 ± 0.5%. Two replicates were tested for each type of mixture. The flow number was defined as the number of cycles required for the asphalt mixtures to exhibit the tertiary flow.

Results and discussions

Model validation

As mentioned previously, the MSCR test data were used for fitting the Prony series and derive the parameters for model inputs. A frequency sweep simulation was performed on the pure SBS-modified asphalt binder and the result was compared with the master curve from the frequency sweep test for the same binder, as shown in Figure 6(a). Results show that the complex moduli from simulations based on MSCR data fit fairly well with those from the experiment. The similar comparisons were conducted for the mastics with 18.9% filler and 16.2% filler, which represent the mastics used in the fine and coarse mixtures, as given in Table 1. The results of the comparison between simulation and frequency sweep test-derived master curves for both mastics are comparable, as shown in Figure 6(b) and 6(c).

The permanent strain after 70 cycles for both fine- and coarse-graded asphalt mixtures obtained from the multi-scale analysis was compared with the creep and recovery curve from the flow number test, as shown in Figure 7. The simulation results without considering the particle contact were also included in the figure to demonstrate how the inclusion of the contact affects the permanent strain curve. Figure 7 clearly shows that by implementing the contact function the prediction power of the multi-scale model on the permanent strain of asphalt mixtures was significantly improved for both fine and coarse mixtures. The predicted permanent strains for the fine and coarse mixtures from modelling after 70 cycles are 11.2% and 7.4% higher than the experimental data respectively, indicating the capability of the model in predicting the permanent deformation of asphalt mixtures at initial cycles of creep loading and recovery.

To further compare the two mixtures in their rutting resistance, the important parameters from modelling, testing and image analysis for both mixtures are summarised in Figure 8(a). Both modelling and experiment show that the permanent strain for the fine mixture after 70 cycles is lower than the coarse mixture. The flow number of the fine mixture is also much higher indicating better rutting resistance. The image analysis clearly demonstrates that the fine mixture has higher total contact length, indicating a better packed aggregate structure relative to the coarse mixture.

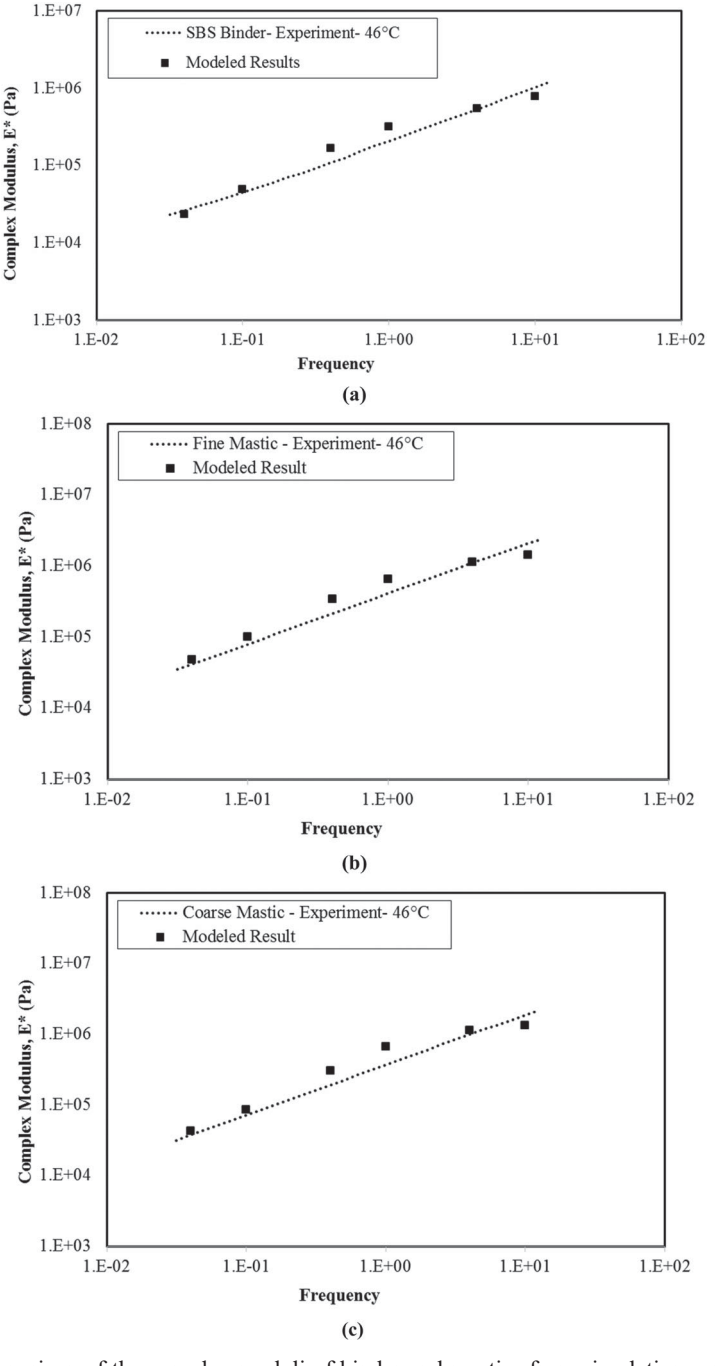

Figure 6. Comparison of the complex moduli of binder and mastics from simulations and experiments: (a) SBS-modified binder, (b) fine mastic with 18.9% filler and (c) coarse mastic with 16.2% filler.

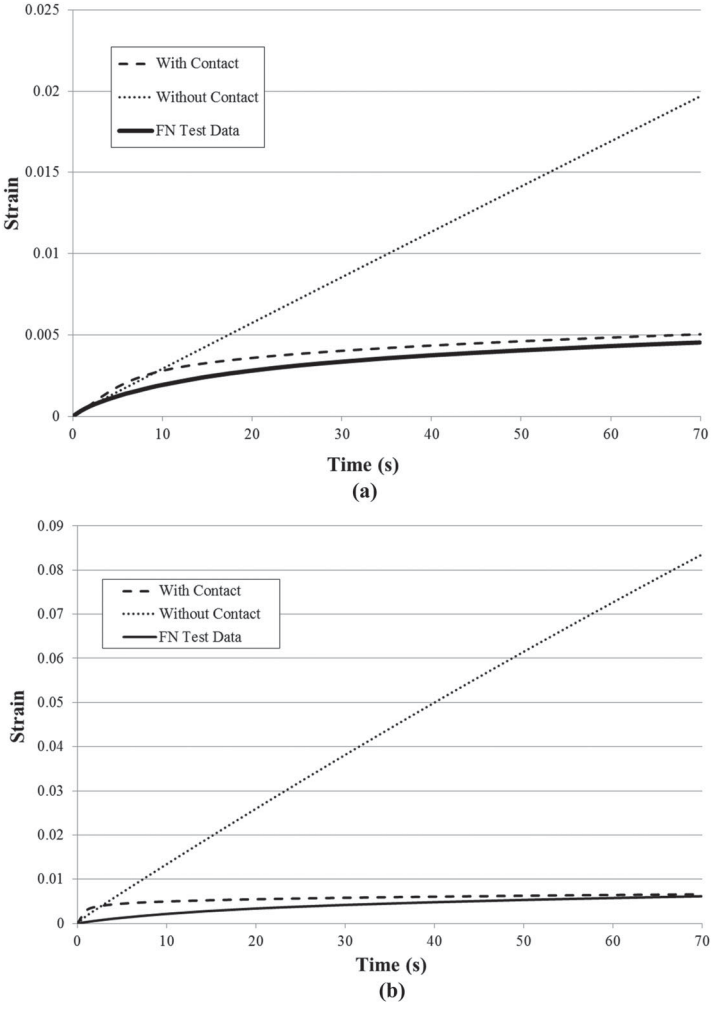

Figure 7. Permanent strain curves after 70 cycles for (a) fine mixture and (b) coarse mixture.

The stress contour plots from the modelling after 70 cycles creep and recovery loading also show that more evenly distributed stress paths exist in the fine mixture than the coarse mixture. Therefore, it is concluded that the fine mixture is more rutting resistant compared to the coarse mixture used in this study.

Multi-scale analysis

In order to obtain the viscoelastic property for the continuous phase (mortar) at the mixture scale, the frequency sweep simulations need to be performed at mastic and mortar scales and the master curves need to be constructed. For all the eight different mixtures used in this study, the master curves for the mastics and mortars are presented in Figure 9. Note that "HJHR-F" refers to the asphalt mixtures with binder of high Jnr and high recovery and the fine-graded aggregates. Similar definitions are used for other seven mixtures.

Key Parameters	Fine	Coarse
Modelled Permanent Strain after 70 Cycles (mm/mm)	0.005038	0.006590
Experimental Permanent Strain after 70 Cycles from FN Test (mm/mm)	0.004532	0.006139
Flow Number (cycles)	430	260
Total Contact Length from iPas2 (mm per 100cm^2)	3055.60	1546.60

(a)

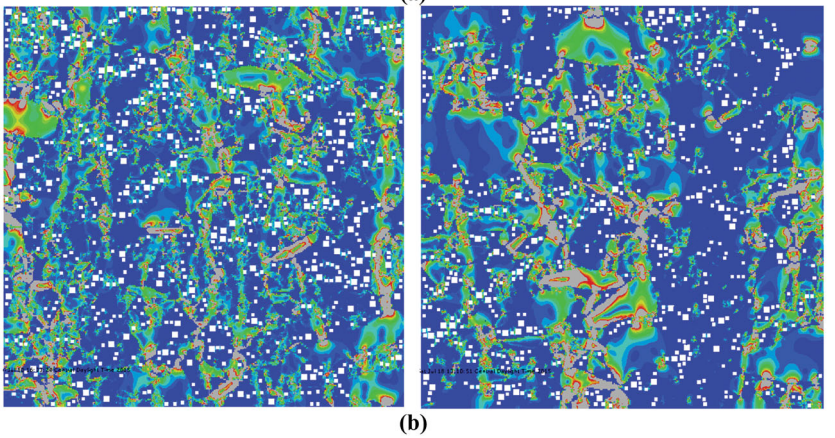

(b)

Figure 8. (a) Comparison of key parameters for fine and coarse mixtures; (b) Von Mises stress contour plots for fine (left) and coarse (right) mixtures.

As shown in Figure 9, the complex moduli of the mastics for the fine mixtures are slightly higher than the ones for coarse mixtures, as in the mastics of fine mixtures the filler content (18.9%) is slightly higher than that of the coarse mixtures (16.2%). Among the mixtures with different binders, the mixtures with HJHR binder have the lowest moduli while the mixtures with LJLR binder have the highest moduli for both fine- and coarse-graded mixtures. Similar trend can be seen when comparing the master curves of mortars for all eight mixtures. Due to the much larger amount of aggregate in the mortar of fine mixtures relative to the coarse mixtures, the complex moduli for the mortar of fine mixtures are much higher than those for the coarse mixtures.

The creep loading simulations were performed at both mastic and mortar scales to define the contact function which was used in the simulation at higher scales. It is interesting to know when the contact between the aggregate particles occurs and how the critical strain at contact affects the permanent strain at the mixture scale. The critical contact strains at both mastic and mortar scales for all mixtures are shown in Figure 10. At the mastic scale, it is found that mastic with lower modulus usually reaches the contact at higher mastic strain. However, the critical contact strains rank differently at the mortar scale. The mortars in the fine mixtures always have lower contact strain relative to the mortars in the coarse mixtures due to the significantly higher volume fraction of aggregates at the mortar scale, which leads to easier contact at lower strain. The contact strains for the mortars for binder with low Jnr are slightly lower than the strains for binder with high Jnr due to its better resistance to deformation. However, the contact strains of mortar for binder with higher recovery are significantly lower than the contact strains for binder with lower recovery even with lower stiffness; this is different from what has been seen at the mastic scale. Compared with the mastic scale, the critical contact for mortar usually occurs after a few cycles of loading. Therefore, there is a possibility that the mortar containing binder with higher recovery has better capability to recover the strain, resulting in lower critical strain at contact.

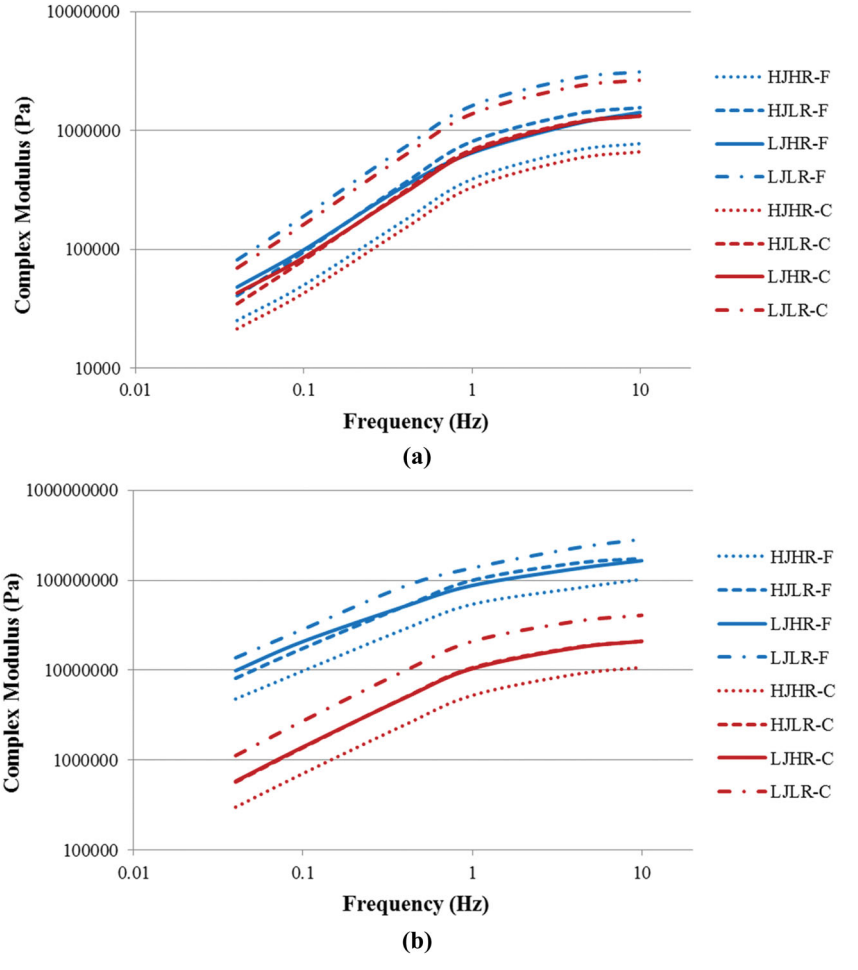

Figure 9. Masters curves of (a) mastics and (b) mortar for all eight mixtures.

Permanent strain analysis

The permanent strains of fine and coarse mixtures with all four binders after 70 loading cycles are shown in Figure 11(a). To investigate the significance of the binder properties and aggregate gradation, an ANOVA analysis on all the mixtures was performed without considering the interactions among the factors, and the result is shown in Figure 11(b).

It is clearly seen that the aggregate gradation is the most dominant factor with the highest significance in the permanent deformation of asphalt mixtures. Also, the viscous component of asphalt binder (Jnr) shows a significant effect, while the elastic component (%*R*) is of no importance overall. The fine mixtures have much lower permanent strains than the coarse mixtures due to much better packing, as discussed above; the mixtures with lower Jnr values have lower permanent strains for both fine and coarse mixtures due to better resistance to permanent deformation of the asphalt binders with low Jnr. The permanent strains for the mixtures with higher %*R* values are lower than the mixtures with lower %*R* values for coarse mixtures; however, almost no effect of the %*R* has been seen for the fine mixtures. The ANOVA analysis was also performed for fine and coarse mixtures respectively, as shown in Figure 11(c) and 11(d). It is

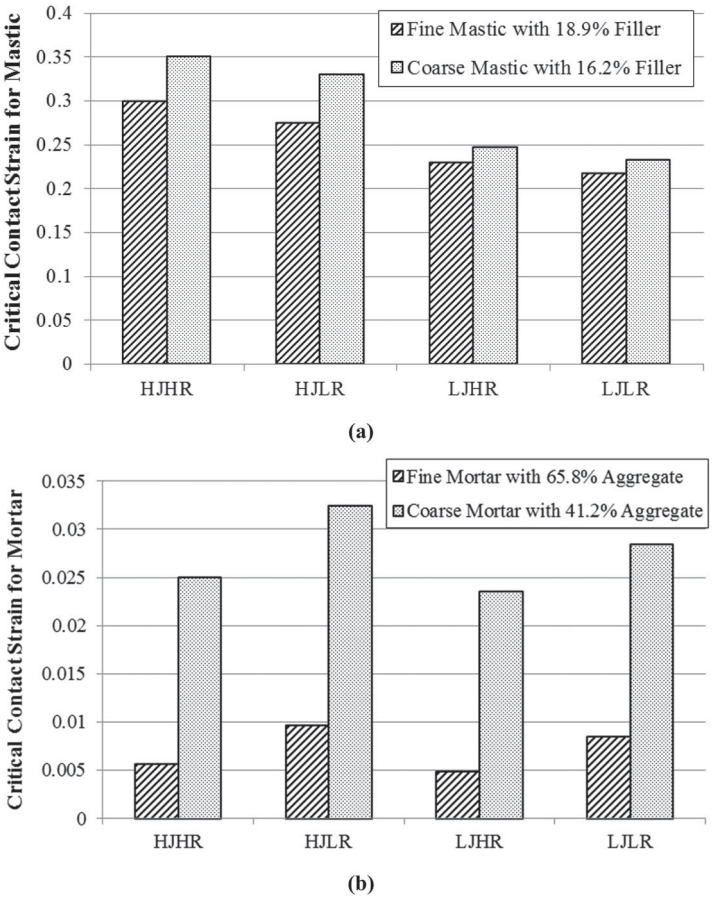

Figure 10. Critical contact strain at (a) mastic scale and (b) mortar scale.

seen that the better packing can reduce the effects of binder viscous and elastic properties on permanent deformation of asphalt mixtures.

The differences of the average permanent strain for all levels of the three factors are also calculated. The average permanent strain of fine mixtures is 26.4% lower than the one for coarse mixtures. The average permanent strain of mixtures with lower Jnr is 13.1% lower than the one for mixtures with higher Jnr. For the coarse mixture, the average permanent strain for mixtures with higher %*R* is about 10.1% lower relative to the one for mixtures with lower %*R*.

The average minimum principal strain (compressive strain) of the continuous phase (mortar) at the mixture scale was also calculated and compared. It can be found that they have identical rankings and trends as the permanent strains of the asphalt mixtures. This is because in the asphalt mixture the aggregates deform very little due to the high stiffness; therefore, the majority deformation of asphalt mixtures results from the deformation of the continuous phase mastic.

Concluding remarks

This paper focused on utilising a recently developed image-based multi-scale modelling technique to evaluate the role of binder properties measured with the MSCR test, and the role of mix

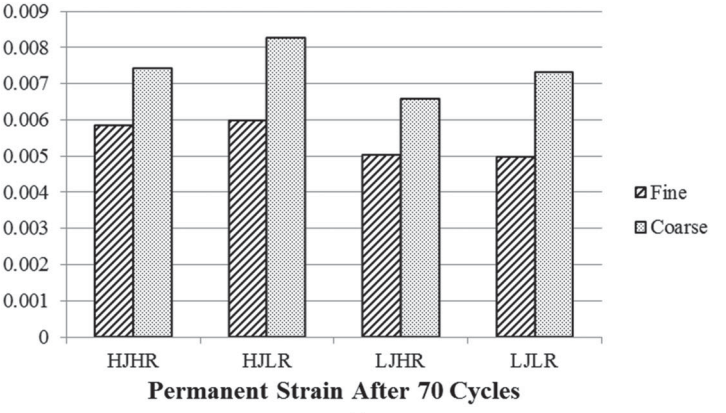

(a)

ANOVA - All Mixtures				
	DF	F-Value	Pr (>F)	Significance
Jnr	1	21.46	0.0098	**
%R	1	4.54	0.1002	
Gradation	1	101.50	0.0005	***
Residuals	4			
R^2_{adj}=94.68%				

(b)

ANOVA - Fine Mixtures				
	DF	F-Value	Pr (>F)	Significance
Jnr	1	75.45	0.0730	.
%R	1	0.11	0.7964	
Residuals	1			
R^2_{adj}=96.08%				

(c)

ANOVA - Coarse Mixtures				
	DF	F-Value	Pr (>F)	Significance
Jnr	1	248.85	0.0403	*
%R	1	193.82	0.0457	*
Residuals	1			
R^2_{adj}=99.32%				

(d)

Figure 11. Permanent strains for (a) all mixtures after 70 cycles, (b) ANOVA for all mixtures, (c) ANOVA for fine mixtures and (d) ANOVA for coarse mixtures.

design in terms of aggregate structure on the permanent deformation of asphalt mixtures. The following remarks summarise the major findings:

(1) The MSCR test results for asphalt binder can be used instead of frequency sweep test to obtain the material input parameters in the multi-scale modelling. The modelled results are validated using binder and mastic master curves as well as the mixture permanent strain curves from the flow number test. The validation indicates the potential effectiveness of using the model to predict the permanent deformation of asphalt mixtures.
(2) The rutting resistance of asphalt mixtures with two different gradations was evaluated through modelling, experimentation and image analysis. Both modelling and experimental results show that the fine-graded asphalt mixture results in lower permanent strain

after 70 loading cycles due to a much better packed aggregate structure, as represented by higher total contact length obtained from the image analysis.

(3) The effects of asphalt binder viscous and elastic properties and aggregate gradations were evaluated through the multi-scale modelling. Results show that the aggregate gradation is the most significant factor affecting the permanent strain of asphalt mixture. The viscous component of asphalt binder (Jnr) also has a significant effect; however, the elastic component (%*R*) is not necessarily important. In a fine-packed mixture, the elasticity has much less influence relative to a coarse-packed mixture.

From the findings presented above, it is concluded that the image-based multi-scale modelling is an effective tool to evaluate the permanent deformation of asphalt mixtures. The authors will continue working on improvement of the contact functions and development of a back-calculation method for stress/strain analysis at multiple scales. Moreover, mixtures with different types of asphalt binders and aggregate gradations need to be tested for model validation. The nonlinearity of the asphalt binder property in the MSCR test will also be considered in the model in the future.

Disclosure statement

No potential conflict of interest was reported by the authors.

References

Arshadi, A., & Bahia, H. (2015). Development of an image-based multi-scale finite element approach to predict mechanical response of asphalt mixtures. *Road Materials and Pavement Design*, *16*(Suppl. 2), 214–229.

Coenen, A. (2011). *Image analysis of aggregate structure parameters as performance indicators of rutting resistance* (Ph.D. Thesis). University of Wisconsin-Madison, Madison, WI.

D'Angelo, J., Reinke, G., Bahia, H., & Marasteanu, M. (2010). Development in asphalt binder specifications. *Transportation Research Circular E-C147*. Transportation Research Board, Washington, DC.

Gierhart, D. (2011). Simple talking points for sharing why your state should be implementing MSCR. Presentation at *SEAUPG MSCR Task Group Web Meeting*.

Golalipour, A. (2011). *Modification of Multiple Stress Creep and Recovery test procedure and usage in specification* (MS Thesis). University of Wisconsin-Madison.

Kong, J., & Yuan, J. (2010). Application of linear viscoelasticity differential constitutive equations in ABAQUS. *Proceedings of 2010 International Conference on Computer Design and Applications, 5*, 152–156.

Ling, C., Hanz, A., & Bahia, H. (2014). Evaluating moisture susceptibility of cold mix asphalt. *Journal of the Transportation Research Record*, *2446*, 60–69.

Ling, C., Moraes, R., Swiertz, D., & Bahia, H. (2013). Measuring the influence of aggregate coating on the workability and moisture susceptibility of cold mix asphalt. *Journal of the Transportation Research Record*, *2372*, 46–52.

Masad, E., Jandhyala, V. K., Dasgupta, N., Somadevan, N., & Shashidhar, N. (2002). Characterization of air void distribution in asphalt mixes using X-ray computed tomography. *Journal of Materials in Civil Engineering*, *2*, 122–129.

Roohi, N., Tashman, L., & Bahia, H. (2012). Internal structure characterization of asphalt mixtures for rutting performance using imaging analysis. *Road Materials and Pavement Design*, *13*(Suppl. 1), 21–37.

Zocher, M. A., Groves, S. E., & Allen, D. H. (1997). A three-dimensional finite element formulation for thermoviscoelastic orthotropic media. *International Journal for Numerical Methods in Engineering*, *12*, 2267–2288.